DOE/ET-53088-120 IFSR #120

STUDY OF GENERALIZED TOROIDAL CUSP CONFIGURATIONS

J. N. Leboeuf
Institute for Fusion Studies
University of Texas

S. T. Ratliff
Lockheed California Company

J. M. Dawson
University of California

January 1984

THEORETICAL STUDY OF GENERALIZED TOROIDAL CUSP CONFIGURATIONS

J. N. Leboeuf
Institute for Fusion Studies
University of Texas
Austin, Texas 78712

S. T. Ratliff
Dept. 72-30, Building 311, Plant B6
Lockheed California Company
P.O. Box 551
Burbank, California 91520

J. M. Dawson
Department of Physics
University of California
Los Angeles, California 90024

ABSTRACT. Hot electrons as well as hot ions are a desirable feature of any fusion device. We investigate by particle simulations (in slab geometry) and simple theory two variants of the Toroidal Cusp Experiment (TCX) with an eye to achieving hot electrons, while retaining its large direct ion heating feature. A toroidal field added to the TCX configuration, with cusp magnets arranged poloidally to partly cancel cusp trapping of the electrons insures electron flow across the cusps and electron heating. Helical winding of the cusp magnets around the torus with pitch $\theta \gtrsim (m/M)^{1/2}$ allows trapped electron flow on average helical paths; however, ions can still flow across the cusps and the $\underset{\sim}{J} \cdot \underset{\sim}{E}$ heating of ions and electrons can be varied at will.

1. INTRODUCTION

A number of surface magnetic field plasma devices in toroidal geometry have been proposed within the last several years [1]. For example, the Polytron concept [1,2], put forth by Haines in 1961, was used to construct a plasma confinement device of the same name at Imperial College, London [3-5]. The device uses poloidal line cusps arranged toroidally on a quartz vessel. The University of California at Los Angeles Toroidal Cusp Experiment (TCX) was constructed in 1981, using the Polytron concept, and is a stainless steel torus (major radius = 45 cm, minor radius = 15 cm) with 48 poloidal line cusps [6,7]. These are only two out of many [1] but both share the interesting property that most of the current is carried by the ions, resulting in large ion heating, while the electrons stay cool and are trapped by the cusp fields.

In TCX for instance, a preliminary plasma discharge is produced by electron emitting tungsten filaments. Voltage applied to the primary side of an iron-core transformer drives a toroidal current through the plasma. The hydrogen/deuterium plasma has the following typical parameters [8]: electron density $n_e = 4 \times 10^{13}$ cm^{-3} (line averaged), ion temperature κT_i = 180 eV - 470 eV, electron temperature = κT_e = 14 eV, transformer loop voltage = 100 V, toroidal current = 5 kA (ion current), and transformer pulse length = 800 μsec.

Our previous theoretical studies [9-12] of TCX were based on a particle point of view using a self-consistent collisionless electromagnetic finite-size particle simulation code, an approximation to TCX in slab geometry. The Polytron device, on the other hand, was primarily modeled with magnetohydrodynamic (MHD) codes [3]. Our

particle simulations showed that a significant fraction of the current, larger than expected from free streaming, is carried by the ions because the electrons, on account of their smaller Larmor radius, are restrained by the cusp fields. The ions get directly heated through $\underset{\sim}{J} \cdot \underset{\sim}{E}$. Our theoretical calculations showed that the electron-to-ion current ratio should scale as $J_e/J_i \simeq (M/m)^{1/2}$ in slab geometry and be equal to 1 in cylindrical geometry. Collisions should reduce this ratio further. The former scaling was verified by our computer simulations. Both our single particle orbit studies and self-consistent simulation studies confirmed the magnetic lens effect of the array of cusps which tends to confine the ions towards the center of the device.

Our purpose here is to investigate two modifications of the TCX configuration so as to possibly allow the electrons to carry some of the current, while retaining its ion focusing properties, its large ion current and direct ion heating. This would result in electron heating and avoid ion cooling by electron-ion collisions. The modifications might also lead to improved confinement although we have not investigated this aspect. The two modifications involve adding a toroidal field [14] to the existing TCX device and also a configuration in which the poloidally placed magnets are rearranged in a helical pattern (giving rise to a configuration similar to the OHTE device [15]). An understanding of the effects of adding these magnetic fields will allow the experimenters to control the relative fraction of electron and ion toroidal and poloidal currents, and electron and ion temperatures. We model the two proposed configurations, approximated in slab geometry, with our standard electromagnetic particle code [16].

Our theoretical calculations are carried out in both the slab geometry of the simulations and in cylindrical geometry (as appropriate for the experiment). Collisions are neglected in this study.

The organization of this paper is as follows. After this introduction, the computer model is briefly reviewed in Section 2. Section 3 describes the results for the helical TCX configuration, while Section 4 contains the results with the addition of a toroidal field to the usual TCX configuration. A summary of the results and conclusions drawn from them are given in Section 5.

2. COMPUTER SIMULATION MODEL

The tool used for our computational studies is a standard two-and-one-half dimensional (two space, x and y, and three velocity and field, x, y, and z, dimensions) electromagnetic finite size particle simulation code [16]. Figure 1 illustrates the relationship between the computer model and the TCX experiment. It represents a toroidal cross section and shows all 48 magnetic cusps. The dotted line indicates the portion of the device which we simulate using the computer model. Slab geometry is used for computational convenience. In the model, the positions and velocities of ions and electrons are computed using the Lorentz force law and Maxwell's equations, applying standard particle simulation techniques [17]. Periodic boundary conditions are used for all field and particle quantities. The transformer produced toroidal electric field in the experiment is modeled in the simulations as a constant electric field in the x direction imposed at every point in space and constant in time. The cusp magnetic field is treated as a constant external field and is

simulated by alternating current strips in the plus and minus z directions located at the upper and lower boundaries of the system in the y direction. The toroidal field is added to the model as a constant magnetic field along the x direction. It can be varied at will in the simulations. The helical configuration (without toroidal field) is modeled by tilting the constant electric field in the x-z plane (x representing the direction across the cusps and z the direction perpendicular to the plane of the cusps), instead of modifying the magnet arrangement which is not possible within the limits of the model.

Typical simulation parameters are as follows: system size $L_x \times L_y = 64\Delta \times 64\Delta$, with the unit grid spacing $\Delta = \lambda_e$, the electron Debye length at $\omega_{pe}t = 0$, with ω_{pe} the electron plasma frequency; particle number, $N_o = 65536$, so that there are 8 particles of each species per cell; collisionless skin depth $c/\omega_{pe} = 5\lambda_e$, with the speed of light $c = 5\ v_{te}$, and v_{te} the electron thermal speed. In the model, the electrons have positive charge and the ions a negative one for historical reasons. The cusp magnetic field is such that the ratio of electron cyclotron frequency ω_{ce} to plasma frequency is $\omega_{ce}/\omega_{pe} = 17.2$ for the maximum field across the cusps; the electron to ion mass ratio is $m/M = 1/20$, the initial temperature ratio $T_e/T_i = 1$; the dc electric field is such that $eE_{dc}/m\omega_{pe}^2\Delta = 0.05$. The evolution of the system is followed in space and time up to approximately 100 ion plasma periods.

3. HELICAL TCX CONFIGURATION

The effect on the plasma behavior of winding the cusp magnets helically around TCX, instead of the present poloidal arrangement, is investigated through single particle orbit calculations and self-constraint particle simulations. The details of the orbit calculation in helical geometry can be found as an Appendix in our own Ref. [11] and the results are only highlighted here for the sake of completeness. In the particle simulations, we mainly concentrate on a detailed investigation of the electron-to-ion current ratio.

3.1. Ion focusing in helical geometry

In cylindrical coordinates for a magnetic field with helical symmetry, the magnetic field and vector potential will depend only on the coordinates r and $u = kz - \ell\theta$, where $L = 2\pi\,\ell/k$ is the pitch of the helix, and λ and k are integers: $\underset{\sim}{B} = \underset{\sim}{B}(r, kz - \lambda\theta)$, $\underset{\sim}{A} = \underset{\sim}{A}(r, kz - \lambda\theta)$.

The equations of motion of ions with charge q and mass M, written as [11],

$$d^2r/dt^2 = q/Mc\ (r\dot{\theta}\ B_z - \dot{z}B_o) + r\ \dot{\theta}^2, \tag{1a}$$

$$d/dt\ (r\dot{\theta}^2) = \frac{qr}{Mc}\ (-\dot{r}B_z + \dot{z}B_r), \tag{1b}$$

$$d^2z/dt^2 = \frac{q}{Mc}\ (B_\theta\dot{r} - r\dot{\theta}B_r), \tag{1c}$$

have a constant of the motion, a kind of helical canonical momentum

$$P_h = kr^2\dot{\theta} + kqA_\theta r/Mc + \ell\dot{z} = \text{constant}. \qquad (2)$$

The constant equals zero if the particle has no helical momentum before entering the magnetic field. The quantities A_θ and c represent respectively the θ component of the vector potential and the speed of light.

The r displacement (assuming zero helical momentum) is given by a solution of Eqs. (1) and (2). Motion close to the z axis, in the limit where B is mostly in the z direction, i.e., $\underset{\sim}{B} = B_o\,\hat{z}$, $B_r = B_\theta = 0$, is described by

$$d^2r/dt^2 + \frac{q^2B_o^2r}{4M^2c^2} - \left(\frac{Lv_z}{2\pi}\right)^2 \frac{1}{r^3} = 0 \qquad (3)$$

The r motion is then that of a simple harmonic oscillator with a $1/r^3$ centrifugal repulsion from the axis because of the particle's angular momentum (zero helical momentum implies some angular momentum). In cylindrical geometry, without helical field, as in the usual TCX configuration (and for zero angular momentum), the r motion is simply described by the first two terms of Eq. (3); i.e., it is a simple harmonic oscillator.

3.2. Electron-ion current ratio for helical TCX configuration

Winding the cusp magnets helically while applying a voltage in the toroidal direction implies that a component of the inductive field will be across the cusps while another component will be along the winding path. We model this situation in the computer model by tilting the direction of the constant electric field E_{dc} away from the x axis. For various angles θ such that $E_{dc} = E_{dc}\,(\hat{x}\cos\theta + \hat{z}\sin\theta)$, we measure the current carried by electrons and ions in various directions. The current across the cusps is given by J_{xe} and J_{xi} for electrons and ions respectively. The current perpendicular to the cusps plane is given by J_{ze} and J_{zi}.

The various measured current ratios are displayed in Fig. 2: J_{ze}/J_{xe} versus θ in Fig. 2a, J_{ze}/J_{zi} in Fig. 2b, and J_{xe}/J_{xi} in Fig. 2c. J_{xe}/J_{xi} and J_{ze}/J_{zi} are approximately constant as θ varies, while J_{ze}/J_{xe} increases as a function of θ. This behavior can be understood as follows. Our previous calculations [9-12] for the usual TCX configuration in slab geometry show that the electrons are restrained from carrying current across the cusps. The free electron acceleration gives an electron current $J_{xe} = N_o e^2 E_{dc} t/m$. The cusps constrain the x motion of the electrons so that their current is proportional to $(m)^{-1/2}$. If the ions are also constrained by the cusps, then their current also is proportional to $(M)^{-1/2}$ [9]. In some of the simulations the ions freely accelerate across the full width of the plasma, in which case their current is proportional to M^{-1}. For the tilted E_{dc}, electrons and ions will carry currents along the x direction given by:

$$J_{xe} \simeq \frac{N_o e^2 E_{dc} \cos\theta t}{m^{1/2}} , \qquad \text{constrained electrons} \qquad (4a)$$

$$J_{xi} \simeq \frac{N_o e^2 E_{dc} \cos\theta t}{M^{1/2}} , \qquad \text{constrained ions} \qquad (4b)$$

$$J_{xi} \simeq \frac{N_o e^2 E_{dc} \cos\theta t}{M} , \qquad \text{unconstrained ions} \qquad (4c)$$

In the x direction they therefore behave the same as in the standard TCX.

In the z direction one might expect the magnetic field to inhibit the electron motion in a similar way. However, z motion causes a charge separation in the y direction and the resulting E field balances the v × B force (the Hall effect) and allows the electrons to freely accelerate in the z direction. The charge separation E_y gives an E × B velocity which is just that needed for freely accelerating electrons in z. There is no way that charge separation fields can give an E × B velocity in the x direction and so the Hall effect cannot cancel the magnetic restraint on the electrons. This is true for the helical electron motion in a helically wound TCX.

Along the z direction, free acceleration prevails and the currents carried by electrons and ions can be written

$$J_{ze} \simeq N_o e \left(\frac{eE_{dc} \sin\theta t}{m}\right) , \qquad (5a)$$

$$J_{zi} \simeq N_o e \left(\frac{eE_{dc} \sin\theta t}{M}\right) . \qquad (5b)$$

The following ratios are then obtained from Eqs. (4a) and (4b), and Eq. (5):

$$J_{xe}/J_{xi} \simeq (M/m)^{1/2} , \tag{6a}$$

$$J_{ze}/J_{zi} \simeq M/m , \tag{6b}$$

$$J_{ze}/J_{xe} \simeq (M/m)^{1/2} \tan\theta . \tag{6c}$$

These estimates are in good agreement with the simulation results as shown in Fig. 2 where the theoretical predictions of Eq. (6) are drawn in as dashed curves. Departures from the theoretical scaling in Fig. 2a are due to the fact that J_{xe} is decreased by a two-stream instability between trapped electrons and streaming electrons, an effect of no consequence to the experiment [12].

These results demonstrate that electrons can be made to carry current parallel to the cusp lines. The implications for an actual device with helically wound cusp magnets are as follows. We want the electron heating to roughly equal the ion heating; thus we want $\underset{\sim}{J}_e \cdot \underset{\sim}{E} = \underset{\sim}{J}_i \cdot \underset{\sim}{E}$ with voltage applied toroidally. In the slab model we can never achieve this. However, for the cylindrical case where the simple theory [9] outlined above predicts $J_{xe} = J_{xi}$ and for various reasons (skin effect and others [18]) is actually less, we can achieve the proper heating ratio by choosing the proper helical angle for the cusp windings. We assume that the toroidal ion current is essentially free acceleration, that the cross helix electron current is zero and that the parallel electron current is given by free acceleration. The desired pitch angle θ, calculated from

$$J_{e\parallel}E_{\parallel} \approx N_o\, e^2\, \frac{E_{dc}^2 t}{m} \sin^2\theta \approx N_o\, e^2\, \frac{E_{dc}^2 t}{M} \approx \underset{\sim}{J}_i \cdot \underset{\sim}{E}\ , \tag{7}$$

is then

$$\theta^2 \approx \frac{m}{M}\ . \tag{8}$$

If the windings are arranged poloidally, i.e., perpendicular to the toroidal direction where the inductive field is applied (θ=0) no electron current will flow; only ion current flows as in the existing TCX setup. If the winding is too loose, then the current will be carried mostly by the electrons, thereby doing away with the ion current and ion heating features. The angle given by Eq. (8) is roughly 1 degree for deuterium and the cusps would advance about 3 cm per turn when wound on a cylinder of 30 cm radius. This is probably too tight and the cusp fields would be extremely weak at the center of the tube. However, in a practical device one probably desires somewhat larger electron heating than ion heating because of the larger electron energy loss rate and angles 3 or 4 times as large would be acceptable.

4. ADDITION OF A TOROIDAL FIELD TO TCX

The addition of a toroidal field to the TCX experiment is being planned for the near future. This is a relatively straightforward experimental procedure. In the simulations, all that is involved is adding a constant magnetic field B_x to the existing fields of the array of cusp. We investigate the effect of varying the toroidal field B_x on the ion focusing through single particle orbit calculations and on the

plasma behavior, in particular the current ratio, by collisionless self-consistent particle simulations.

4.1. Single particle ion orbits in combined toroidal and cusp fields

We wish to investigate the phenomenon of ion focusing with varying toroidal field magnitude. Single particle orbits of a class of ions with initial drift velocity in the x direction $v_{di}/\omega_{pe}\Delta = -1.0$ and initial positions x=0 and $L_y/6 \leq y \leq 5L_y/6$ are followed in space and time in the combined toroidal and cusp fields, with the dc electric field and self-consistent fields set equal to zero in the code of Section 2. The results are presented in Fig. 3. The changes in magnetic field topology from the initial TCX configuration (with $B_t/B_c = 0$) for $B_t/B_c = 0.03$ and $B_t/B_c = 0.3$ (where B_t is the magnitude of the toroidal field B_x and B_c is the maximum cusp field strength) are displayed in Figs. 3a, b, and c, respectively. The corresponding ion orbits are displayed alongside in Figs. 3d, e, and f. We note the change in topology from an array of cusps with two nulls, to one with one null and finally to a mirror configuration. Ion focusing is strongest in the absence of toroidal field, in which case the orbits close to the center of the cusp array have the following equation of motion (simple harmonic oscillation) and focusing period [11]:

$$d^2y/dt^2 + \frac{q^2\langle B_x^2\rangle}{M^2c^2}\, y = o \ , \tag{9a}$$

$$\tau = \frac{2\pi Mc}{(q\langle B_x^2\rangle)^{1/2}} \ , \tag{9b}$$

where $\langle B_x^2 \rangle$ is the cusp field evaluated at $y = L_y/2$, averaged over one x period. The simulation period is $\omega_{pi}t = 140$, in agreement with Eq. (9b). As is apparent from Fig. 3, focusing still occurs for the other values of B_t/B_c but the period is lengthened considerably and the focusing radius increased as B_t/B_c increases. We might expect some deterioration of ion confinement in the experiment as the toroidal field is increased, and the ions are less well focused away from the cusps and the walls towards the center of the device. However, the dependence of confinement on B_t has not been investigated in detail.

4.2. Self consistent simulations of TCX with toroidal field

The original premise was that a toroidal field would partly cancel the cusp trapping of the electrons and allow them to carry more of the current. It was tested with the code and parameters of Section 2, i.e., with dc electric field and self consistent fields on. We shall see that this expectation is not necessarily true.

We first consider in some detail the case with $B_t/B_c = 0.03$ of Fig. 3b, where a single null remains out of the original two. The evolution of the field lines is displayed in Fig. 4a at $\omega_{pi}t = 0$, 4b at $\omega_{pi}t = 11$, and 4c at $\omega_{pi}t = 22$. The configuration is not greatly modified in time. Stretching of the field lines along the positive x direction is, however, apparent. This indicates that the electrons, trapped by the cusp fields on account of their small Larmor radius, and feeling the force of the dc electric field, stretch the field lines [9]. Note that some of the field lines have reconnected and now run along the x axis at the center of the system.

We have monitored the electron-to-ion current ratio as a function of time in this case. It is drawn in Fig. 5, along with its counterpart with $B_t = 0$. The current ratio for $B_t = 0$ is $J_e/J_i = (M/m)^{1/2}$. The electrons carry less current in the case of one null only since J_e/J_i stands at 80% of the usual TCX value. The configuration of Fig. 3b therefore makes for a better electron trap. The ions drift velocity is about the same with or without toroidal field.

The effect of varying the toroidal field strength B_t on the electron-to-ion current ratio is best illustrated in Fig. 6. We plot the value of J_e/J_i at $\omega_{pi}t = 22$ (steady state value) as a function of B_t/B_c. With no toroidal field, the ratio is $J_e/J_i = (M/m)^{1/2}$. Fig. 6 shows that J_e/J_i does indeed start from $(M/m)^{1/2}$ when $B_t = 0$, but is reduced for $0.03 < B_t/B_c < 0.1$, being minimum for $B_t/B_c = 0.03$; the case analyzed in detail in Figs. 4 and 5. Thereafter, the current ratio increases, reaching a value of $0.5(M/m)$ for the mirror configuration of Fig. 3c with $B_t/B_c = 0.3$.

The scaling of the current for the mirror-like configuration can be explained as follows. The reduction of the electron current is not attributable to the cusp field trapping the electrons but more to mirroring of those electrons with pitch angle such that $\sin^2\theta > 1/R = B_o/B_m$ with mirror ratio R, bulge and throat fields B_o and B_m, respectively. The electrons with $\sin^2\theta < 1/R$ will simply free stream. The ratios of mirror-reflected electrons N_r and of free-streaming electrons N_s to the total number of electrons N_o are given by [19]

$$N_r/N_o \simeq (1 - 1/R)^{1/2} , \tag{10a}$$

$$N_s/N_o = 1 - (1 - 1/R)^{1/2} . \tag{10b}$$

On the other hand, the ions are non adiabatic and are not stopped by the mirrors; the ions free stream and carry a current $J_i = N_o e^2 E_{dc} t/M$. Only the free-streaming electrons carry a current, so that $J_e = N_s e^2 E_{dc} t/m$, and the current ratio for such mirror-like configurations is

$$J_e/J_i \simeq (N_s/N_o) \frac{M}{m} \simeq \left[1 - \left(1 - \frac{1}{R}\right)^{1/2}\right] \frac{M}{m} . \tag{11}$$

The measured mirror ratio in the simulations is $1/R = B_o/B_m = 4.2/5.45 = 0.77$, so that $N_s/N_o = 0.52$ and $J_e/J_i \simeq 0.5(M/m)$, in excellent agreement with the simulation results of Fig. 6 for $B_t/B_c = 0.3$.

The implications of these results for the experiment are as follows. We can consider the toroidal field strength at which the electrons carry more current than they do without toroidal field in the slab geometry of the simulation as an estimate of the strength needed for the electrons to carry any current at all in the experiment. Namely, the toroidal field should be sufficiently larger than the one required to suppress one null out of two for the electrons to do so.

5. DISCUSSION

The Toroidal Cusp Experiment presently operates in such a way that the inductive field from the transformer only accelerates ions across the cusps and hence only yields ion toroidal current (within experimental accuracy) and ion heating. While the simulations performed here are only rough approximations in slab geometry to the experimental environment, they enable us to infer that helically wound cusp magnets need only be wound by an angle $\theta \simeq (m/M)^{1/2}$ away from the poloidal, about 1 to 4 degrees, for the power input to electrons and ions to be equal. The TCX configuration with a toroidal field of such strength so as to suppress one null out of two (approximately 10 G in TCXI) results in better electron trapping and reduced electron current. For the electrons to start carrying some of the current (they carry none to date within the experimental accuracy) the toroidal field needs to suppress the cusp field over a large fraction of the minor radius. For a maximum cusp field of 1.5 kG, the simulations point to a toroidal field of 100-300 G for a significant fraction of electron current, at least in the absence of collisions. Higher toroidal fields which would turn the configuration into an array of mirror cells should be avoided; such EBT like mirror cells, without hot electron ring stabilization would be MHD unstable [20]. On the other hand, if stabilization could be achieved with substantial direct ion heating the configuration would be very interesting.

Both in the helical configuration and the configuration with toroidal field, there is a lessening of the focusing effect, i.e., longer focal length or period and larger focal area. This could lead to a reduction in the ion confinement by not forcing the ions far

enough away from the cusps. On the other hand, there is definite energy confinement in TCX and we cannot really say at this time that a reduced confinement will occur. In the end, what we would really like to do is close off the escaping field lines, at least for a large part of the plasma, to eliminate direct electron energy loss. This might be accomplished by pulsing on additional external fields (perhaps θ pinch-like) once the ions reach thermonuclear temperatures. Even if the electrons are lost, however, a hot ion plasma in an upgraded TCX device run in a quasistationary fashion (applying AC to the transformer) can be useful for engineering and materials studies.

ACKNOWLEDGEMENTS

The authors would like to thank G.W. Shuy for suggesting investigation of the TCX configuration with a toroidal field, and M. Rhodes and N. C. Luhmann, Jr., for many stimulating discussions. This work was supported by the United States Department of Energy Grants DE-AM03-768F0010 PA26, Task VIB at UCLA and DE-FG05-80ET 53088 at IFS.

REFERENCES

1. HAINES, M.G., Nucl. Fusion 17 (1977) 811.

2. HAINES, M.G., in Plasma Physics and Controlled Nuclear Fusion Research (Proc. Conf. Salzburg, 1961) Nucl. Fusion 1962 Supplement, Part 3, IAEA, Vienna (1963) 1122.

3. KILKENNY, J.D., DANGOR, A.E., HAINES, M.G., Plasma Phys. 15 (1973) 1197.

4. CHAQUI, H., DANGOR, A.E., HAINES, M.G., KILKENNY, J.D., Plasma Phys. 23 (1981) 287.

5. KILKENNY, J.D., Ph.D. Thesis, University of London (1972).

6. RHODES, M., DAWSON, J.M., LEBOEUF, J.N., LUHMANN, N.C. Jr., Phys. Rev. Letts. 48 (1982) 1821.

7. RHODES, M., Ph.D. Thesis, University of California, Los Angeles (1982).

8. RHODES, M., University of California, Los Angeles, Private Communication (1983).

9. LEBOEUF, J.N., RATLIFF, S.T., DAWSON, J.M., RHODES, M., LUHMANN, N.C. Jr., Phys. Fluids 25 (1982) 2045.

10. RATLIFF, S.T., Ph.D. Thesis, University of California, Los Angeles (1982).

11. RATLIFF, S.T., LEBOEUF, J.N., DAWSON, J.M., RHODES, M., LUHMANN, N.C. Jr., Nucl. Fusion 23 (1983) 987.

12. RATLIFF, S.T., DAWSON, J.M., LEBOEUF, J.N., Phys. Rev. Letts. 50 (1983) 1990.

13. WATKINS, M.L., POTTER, D.E., KILKENNY, J.D., HAINES, M.G., DANGOR, A.E., in Plasma Physics and Controlled Nuclear Fusion (Proc. 4th Int. Conf. Madison, 1971) Vol. 1, IAEA, Vienna (1971) 621.

14. SHUY, G.W., Science Applications Inc., Private Communication (1982).

15. OHKAWA, T., CHU, M., CHU, C., SCHAFFER, M., Nucl. Fusion 20 (1980) 1464.

16. LEBOEUF, J.N., TAJIMA, T., DAWSON, J.M., Phys. Fluids 25 (1982) 784.

17. DAWSON, J.M., Rev. Mod. Phys. 55 (1983) 403.

18. RATLIFF, S.T., DAWSON, J.M., Phys. Fluids 27 (1984) 1743.

19. TAJIMA, T., DAWSON, J.M., Nucl. Fusion 20 (1980) 1129.

20. VAN DAM, J.W., LEE, Y.C., In EBT Ring Physics (Proc. Workshop Oak Ridge, 1979) (1979) 471.

FIGURE CAPTIONS

Fig. 1

Relationship between the TCX plasma device and the computer model. The toroidal cross section of TCX shows all 48 cusps and the dotted lines show the portion of the device that we simulate. The coordinate system of the computer model is also shown.

Fig. 2

TCX simulation with tilted dc electric field as an approximation to the helical TCX configuration. (a) Ratio of electron currents perpendicular to and in the plane of the cusps as a function of tilt angle θ. (b) Electron-to-ion current ratio perpendicular to the cusps plane as a function of tilt angle θ. (c) Electron-to-ion current ratio across the cusps as a function of tilt angle θ.

Fig. 3

TCX simulation with a toroidal field. Magnetic field topologies for various values of B_t/B_c. (a) $B_t/B_c = 0$. (b) $B_t/B_c = 0.03$. (c) $B_t/B_c = 0.3$. Single particle orbits in the x-y plane for (d) $B_t/B_c = 0.0$, (e) $B_t/B_c = 0.03$, and (f) $B_t/B_c = 0.3$.

Fig. 4

TCX simulations with a toroidal field. Time evolution of the magnetic field lines for $B_t/B_c = 0.03$ at (a) $\omega_{pi}t = 0$, (b) $\omega_{pi}t = 11$, and (c) $\omega_{pi}t = 22$.

Fig. 5

TCX simulation with toroidal field. Toroidal electron-to-ion current ratio as a function of $\omega_{pi}t$. The solid curve is for $B_t/B_c = 0.03$, the dashed curve for $B_t/B_c = 0$. The dotted line represents the theoretical estimate for $B_t/B_c = 0$.

Fig. 6

TCX simulation with toroidal field. Toroidal electron-to-ion current ratio as a function of B_t/B_c. The dots indicate the simulation values. The dashed lines represent the theoretical estimates.

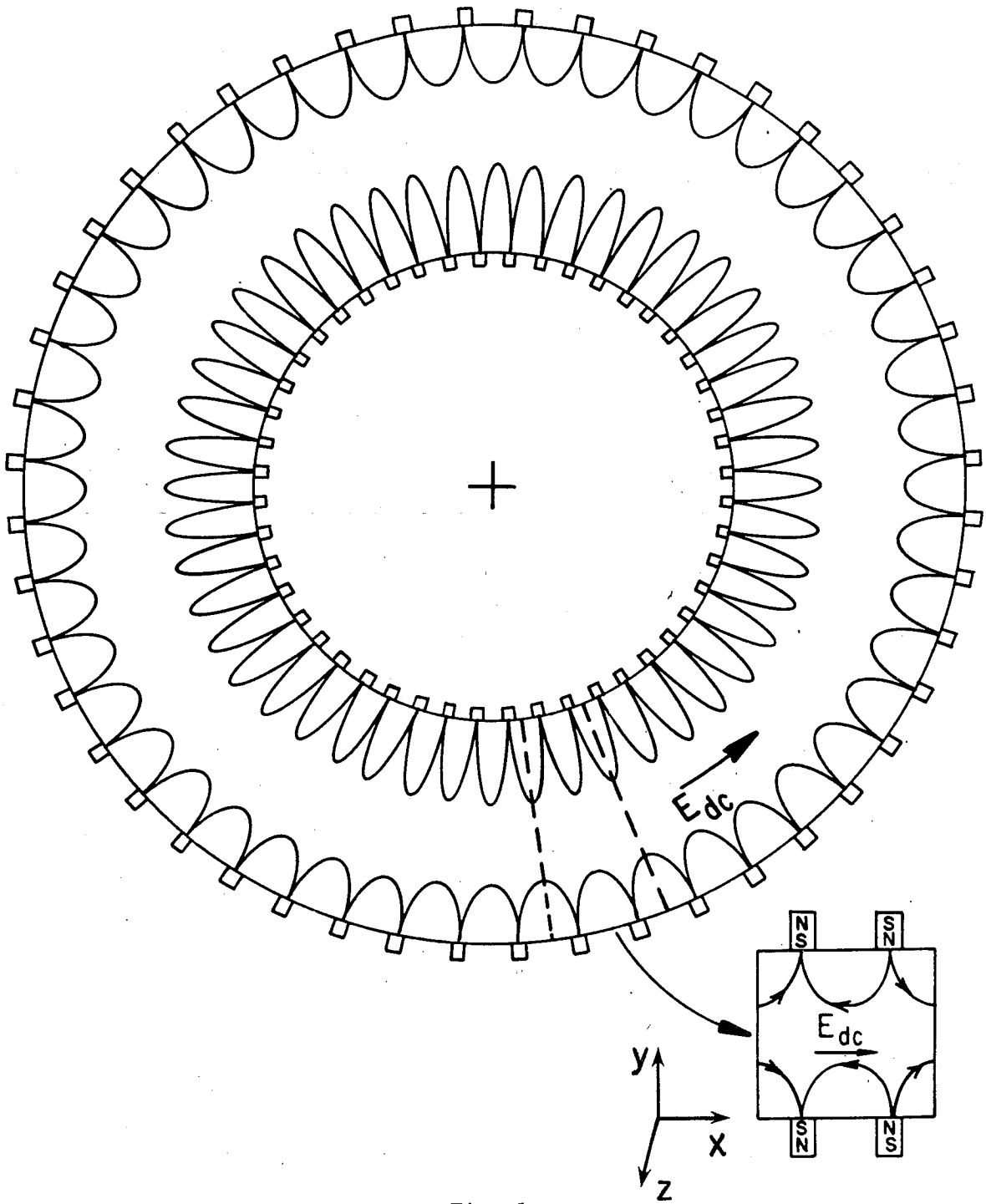

Fig. 1

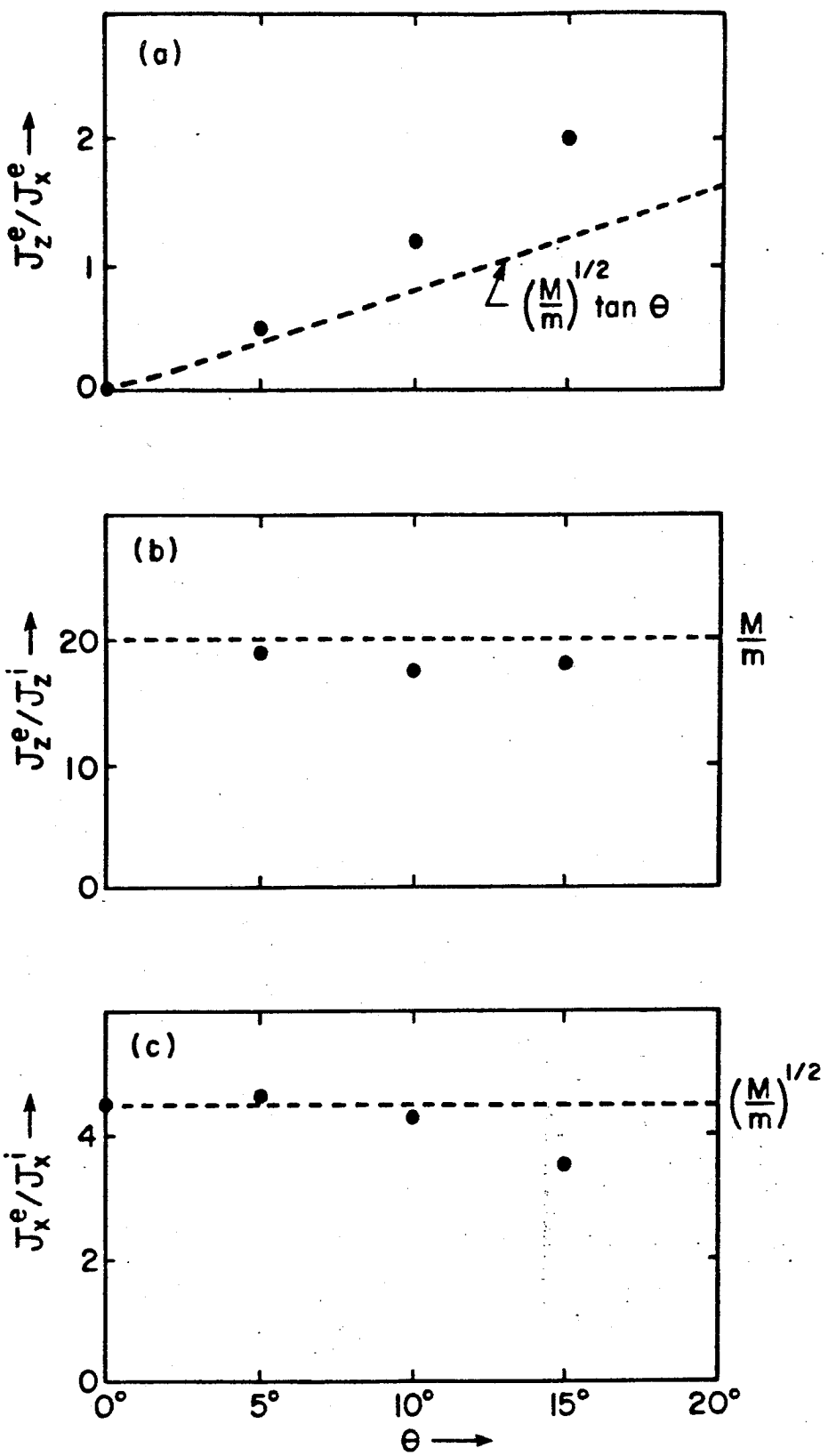
(a)
J_z^e/J_x^e
2
1
0
$\left(\frac{M}{m}\right)^{1/2}$ tan θ
(b)
J_z^e/J_z^i
20
10
0
$\frac{M}{m}$
(c)
J_x^e/J_x^i
4
2
0
$\left(\frac{M}{m}\right)^{1/2}$
0°
5°
10°
15°
20°
θ

Fig. 2

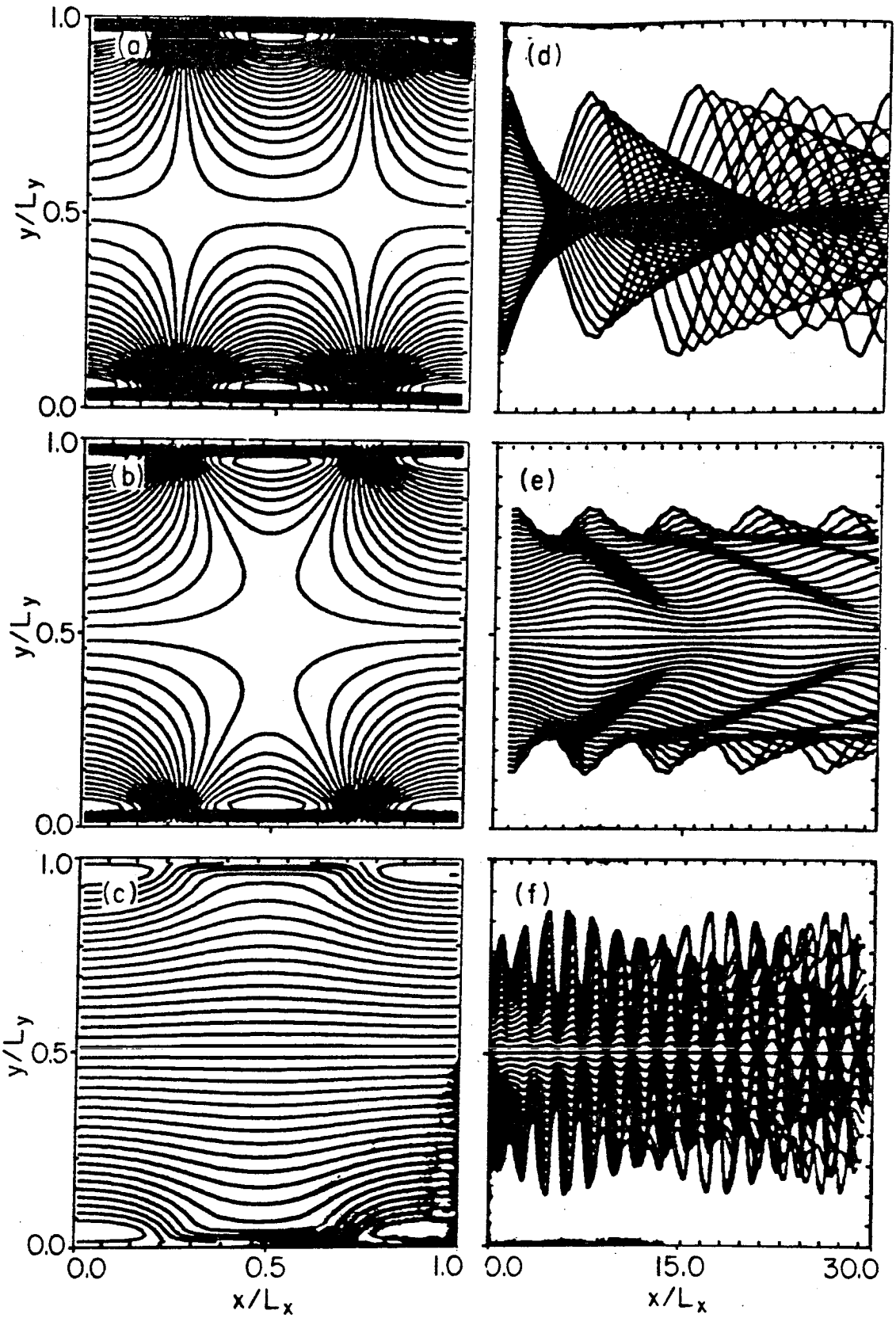

Fig. 3

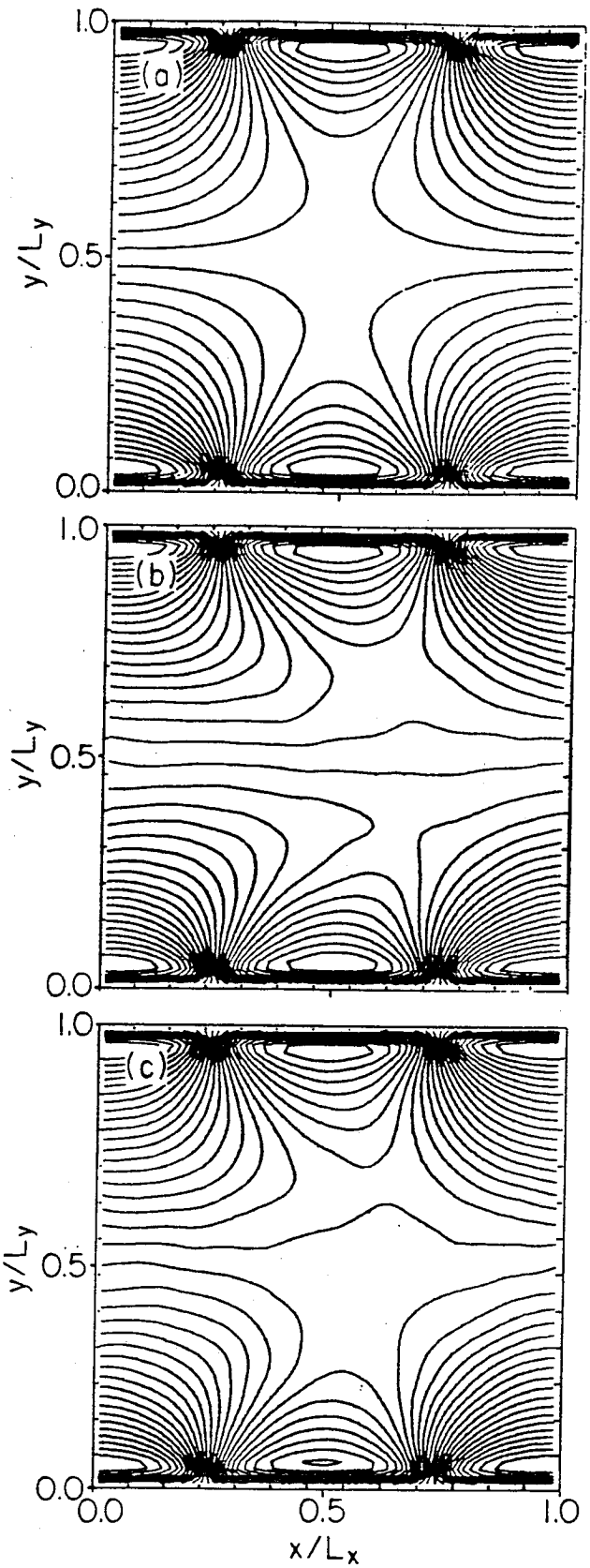

Fig. 4

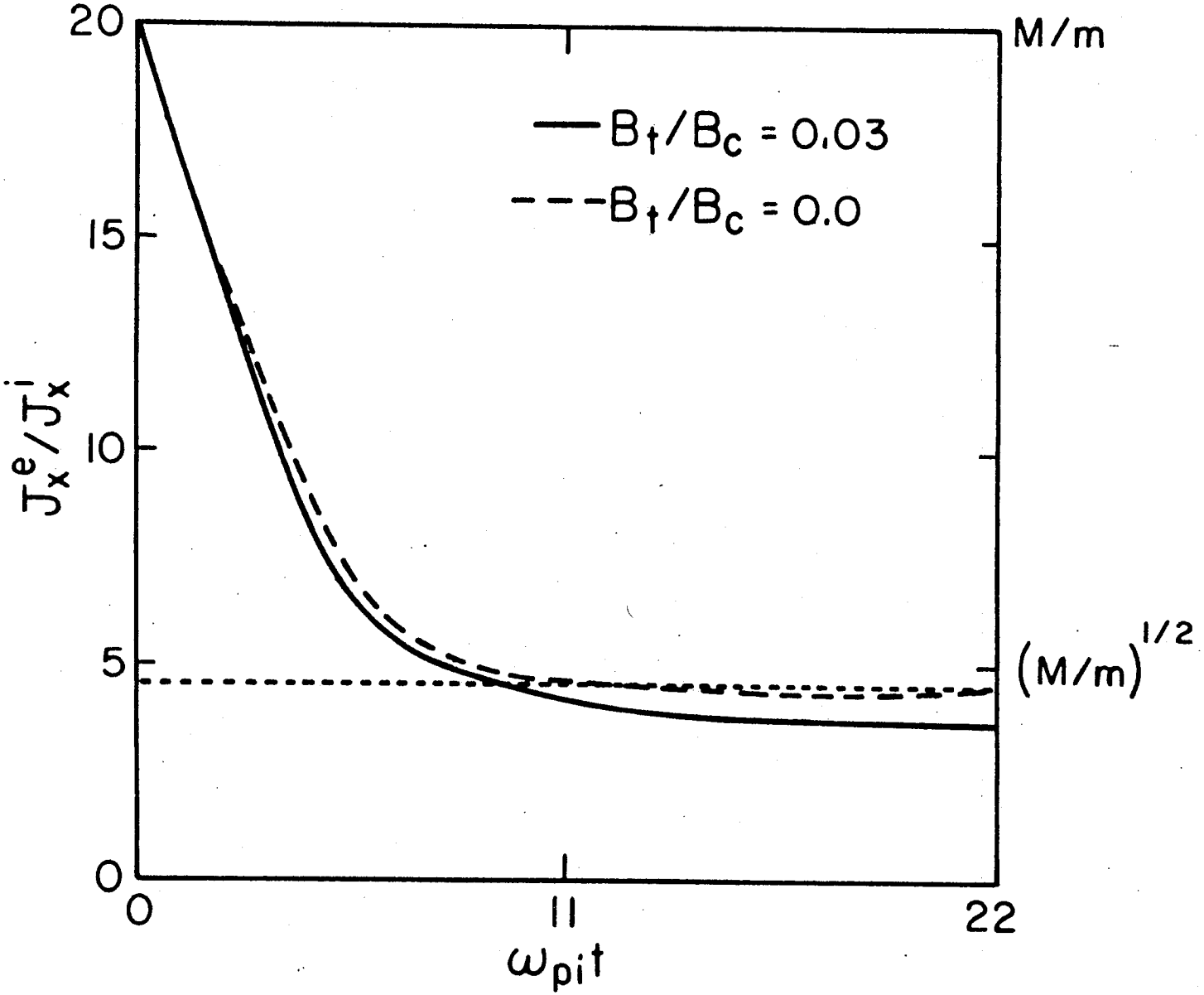

Fig. 5

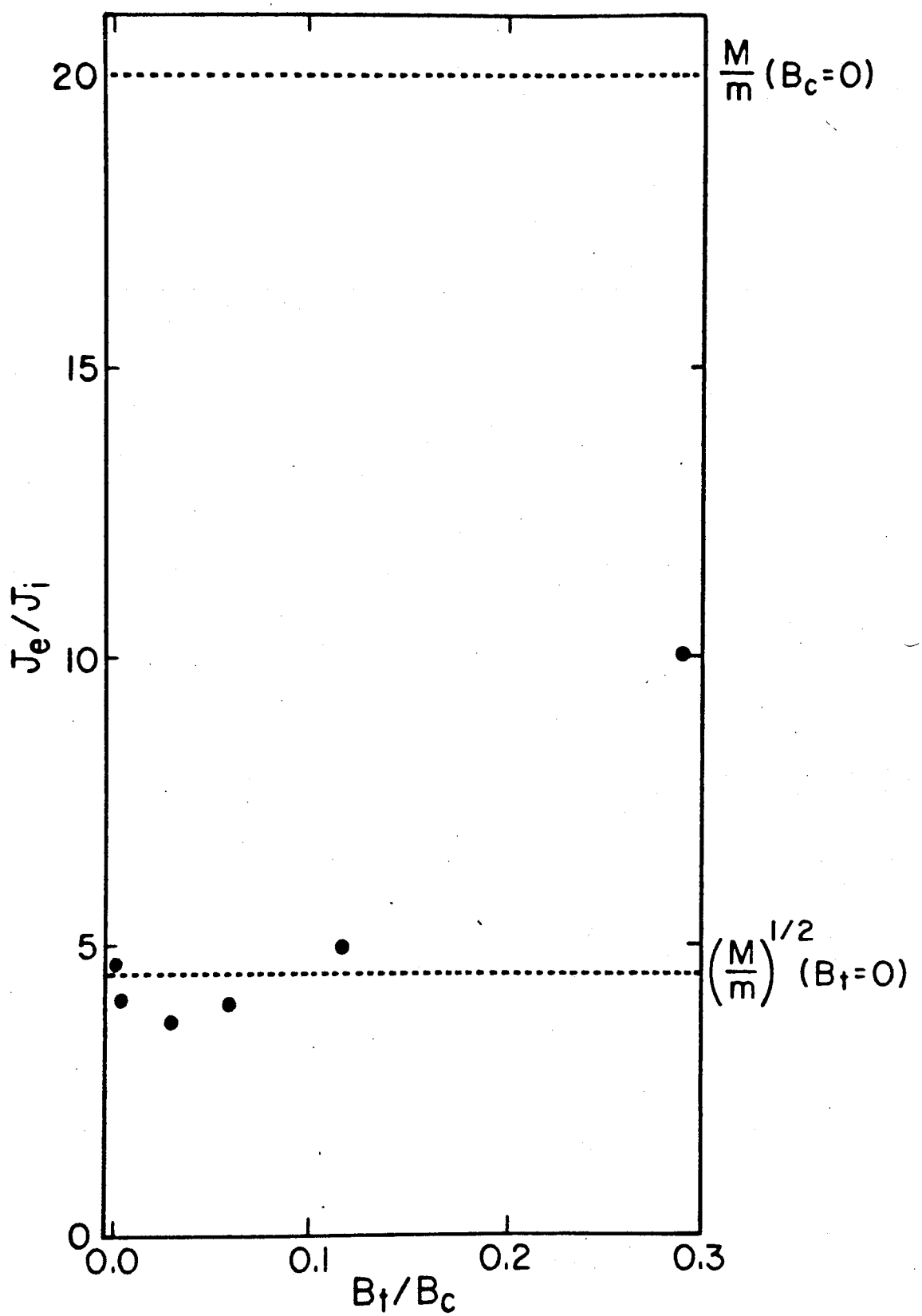
20
15
10
5
0
J_e/J_i
$\frac{M}{m}(B_c=0)$
$\left(\frac{M}{m}\right)^{1/2}(B_t=0)$
0.0
0.1
0.2
0.3
B_t/B_c

Fig. 6